Computations of SAR Distributions for Two Anatomically Based Models of the Human Head Using CAD Files of Commercial Telephones and the Parallelized FDTD Code

Adam D. Tinniswood, Cynthia M. Furse, and Om P. Gandhi, *Fellow, IEEE*

***Abstract*—A method for importing data from computer-aided design (CAD) files for a mobile telephone into finite-difference time-domain (FDTD) simulation software is described. Although the FDTD method is well suited for the bio-electromagnetic simulations and has become the method of choice for most researchers in this area, there may be some limitations to its use. Limitations include, the description of the source (e.g., the mobile telephone) and the fact that the FDTD method requires large amounts of memory and computational power. The size of the computational space is dependent upon both the physical size of the model and its resolution. Higher frequencies of operation require higher resolutions. This could place the solution of some problems outside the capabilities of the technique. Often the telephone has to be represented by a plastic covered metal box, which approximates the shape of the actual device. The paper addresses these problems. Wires and circuit boards inside the telephone can act as resonant elements if they are not shielded. This potential problem is also considered. The large problem size associated with high-resolution FDTD simulations is accommodated by the use of a parallel implementation of the FDTD method (run on an IBM SP-2). The techniques developed here are used for two anatomically based head models that have been developed from magnetic resonance imaging (MRI) of two human subjects. The usefulness of the techniques developed and comparisons of the specific absorption rates (SAR's) in the two models are discussed.**

I. Introduction

THE United States Federal Communications Commission has adopted a modified version of the ANSI/IEEE C95.1-1992 R.F. safety guidelines [1], which limit human exposure to electromagnetic (EM) fields from mobile communication devices [2]. In short, the mass normalized rate of energy absorption (SAR) is limited to 1.6 W/kg averaged over any 1 g of tissue.

Of particular interest for this paper, is the level and distribution of SAR in the human head and the methods by which this can be determined. The are two general approaches to the determination of the SAR distribution in human tissue, by physical measurement or numerical simulation. This paper concentrates on the numerical approach and discusses methods for overcoming some of the limitations of numerical modeling.

Manuscript received March 3, 1997; revised January 22, 1998.

The authors are with the Department of Electrical Engineering, University of Utah, Salt Lake City, UT 84112 USA.

Publisher Item Identifier S 0018-926X(98)04310-5.

The method of choice for the numerical simulation of bio-electromagnetic problems is the finite-difference time-domain (FDTD) method [3], [4]. The use of the FDTD method in bioelectromagnetics is well established as it is well suited to the modeling of electromagnetic wave propagation through dielectric materials. As each point in the three-dimensional (3-D) FDTD problem space can have a different dielectric property, complex dielectric systems can be modeled. This type of approach is ideal for systems such as the human head or the body. Models of the dielectric structure have been developed by the segmentation of magnetic resonance imaging (MRI) scans. Studies to determine the dielectric properties of each of the tissues have been carried out [5] and, using this data, an accurate simulation of field distributions in the body is possible.

The mobile communication devices on the market in the United States at the present time operate in two different frequency bands centered upon 835 and 1900 MHz. For accurate simulation at these high frequencies, millimeter resolution models of the human head are required [6]–[8]. However, the use of higher resolution models becomes difficult as the amount of memory for computer simulation prohibits their use. A parallel FDTD algorithm has been devised for use on high-performance supercomputers, which allows the simulation of much higher resolution problems. Methods of processing and visualizing the large amount of data produced by these simulations have also been developed.

A commonly used method for representing the mobile telephone in the simulation is to use a plastic-coated metal box of similar size to the original telephone. By careful sizing and positioning of the antenna, near-field radiation patterns can be found in close agreement with measured patterns [8]–[10]. In this paper, a new method is introduced that allows the use of CAD files employed in the design of the telephone. Tools have been developed which convert the descriptions in these files to a 3-D image that can be used as a model in the simulations. This approach provides a greater accuracy in simulation and reduces the time required to set up a simulation significantly. It also allows proper modeling of the partial shape and size of the metal box used for shielding the microwave source, and shape, size and locations of the various buttons used for dialing. Furthermore, it is also possible to examine the effect

Fig. 1. A test telephone as imported from the CAD file (resolution: 1.974 $\times$ 1.974 $\times$ 3.0 mm).

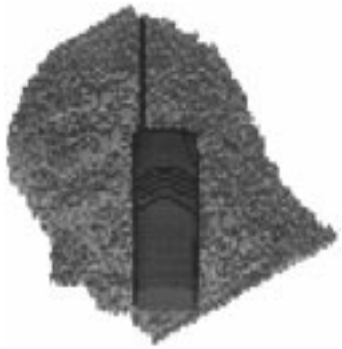

Fig. 2. The telephone next to the head model.

of any resonant type circuits that may occur in such unshielded regions in the SAR distributions.

II. CAD Input of the Mobile Telephone

While the accurate anatomically based descriptions of the human body have been developed, with the use of MRI scans, the description of the device is still described as a plastic-coated metal box. To overcome this limitation, CAD files have been used to generate a description of the telephone.

The CAD file is scanned to find the outline of the telephone structure, giving the general profile of the device. This profile is then resampled to provide a 3-D matrix, which can be used in the FDTD simulation (Fig. 1). The inside of the profile is considered as metal and this is then coated with plastic. Owing to the limitations of resolution, a reduced dielectric constant is used in line with the method described in [10], [11]. Difficulties were found in describing the buttons from the CAD file and, thus, a number of plastic buttons have been added manually.

Simulations with both a telephone input from a CAD file and a telephone made up of an idealized plastic-covered rectangular metal box of a similar size have been carried out. In both cases $\lambda/4$ and $\lambda/8$ monopole antennas have been used. The 1.974 $\times$ 1.974 $\times$ 3.0 mm resolution anatomically-based model of the head [4] has been used in these simulations although no hand has been placed around either telephone (Fig. 2).

III. Head Models

Two head models have been used in this work, the first of which is described in [11] and the second derived in a similar way. The first model has been classified into voxels of dimensions 1.974 $\times$ 1.974 $\times$ 3.0 mm (Fig. 2) and the second into voxels of size 0.9375 mm along each of the orthogonal axes. For accurate simulation using these data sets electrical properties have been prescribed for each of the classified tissues [4], [5]. A list of the classified tissues, their electrical properties and the assumed mass densities can be found in [11].

The 1.974 $\times$ 1.974 $\times$ 3.0 mm has been over sampled to produce a third model with voxels of dimensions 0.987 $\times$ 0.987 $\times$ 1.0 mm. The weights of individual tissues for each of the three models compare well with those given in [13]. The dimensions of each of the models together with the size of the FDTD problem space required to include the telephone are given in Table I.

TABLE I
Model and Simulation Size for the Three Head Models

	Model 1 1.974×1.974×3.0mm	Model 2 0.987×0.987×1.0mm Re-sampled from model 1	Model 3 0.9375mm^3
Model Size (voxels)	103×114×85	206×228×225	202×243×282
Problem Size including source (Voxels Required).	153×154×130	265×258×290	256×259×300
Memory Requirement	110 MBytes	713 MBytes	716 MBytes
Solution Time single workstation*	60 min.	36 hr. (est.)	36 hr. (est.)
Solution Time on 1 node (at 1900MHz)**	63 min.	37 hr. (est.)	37 hr. (est.)
Solution Time on 2 nodes (at 1900MHz)**	32 min.	18.5 hr. (est.)	19 hr. (est.)
Solution Time on 4 nodes (at 1900MHz)**	17 min.	9.5 hr.	9.7 hr. (est.)
Solution Time on 8 nodes (at 1900MHz)**	9 min.	4.7 hr.	5.0 hr.
Solution Time on 16 nodes (at 1900MHz)**	5.25 min.	2.8 hr.	2.9 hr.

* HP C160
** of IBM SP-2.

Table I also gives the solution time on a single workstation (HP 755) and on 1, 2, 4, 8, and 16 nodes of the IBM SP-2 super computer. Simulations using models 2 and 3 cannot be run on a normal workstation, due to the amount of memory required. However, an estimated time is given for a workstation with sufficient memory.

IV. A Parallel Algorithm

One method that can be used to increase the capability of an existing numerical technique is to adapt it to run on a parallel processing platform. Although many types of parallel processing platforms exist, it is the coarse grain distributed memory architecture that is of relevance to this work. The parallelization of the FDTD algorithm has been carried out with two aims: first, that it should be useful for simulation of bioelectromagnetic problems and second, that it be optimized

for very large problems. The FDTD algorithm is well suited to solution on distributed memory parallel processing systems as the field components on one cell of the geometry can be evaluated from fields on the adjacent cells, i.e., there is only a local data requirement. The 3-D problem space can be divided into smaller subvolumes. An individual processor can then compute the fields inside each subvolume, providing a small amount of data is communicated from neighboring processors. Communication is only required for FDTD cells along the surfaces of these subvolumes. Consequently the amount of communication is proportional to the surface area of the subvolumes, whereas the computational load of each processor is based upon their volume.

For a problem of significant size, therefore, the ratio of computation to communication is very high, resulting in an efficient parallel algorithm. The efficiency can be maximized by choosing an appropriate topology to suit the dimensions of the FDTD problem space. The volume-to-surface area is optimal (i.e., highest) when the subvolumes are cubic.

In general, the following quantities are required to examine the distribution of SAR's within the head and neck.

- Peak E-fields.
- SAR values at all points in the FDTD problem space.
- Peak SAR value for a single voxel.
- Peak 1-g averaged SAR value.
- Power radiated from the FDTD problem space.
- Power absorbed by all dielectrics within the FDTD problem space.
- Volume averaged SAR values for individual tissues within the FDTD problem space.

The actual FDTD simulation calculates the peak E-fields and the power radiated from the external FDTD grid. The remainder of the required quantities are computed using a post processor, which also runs on the parallel machine. The reasoning behind this is that these remaining quantities, with the exception of the 1-g averaged SAR, can be computed on a cell-by-cell basis. The amount of memory used in the FDTD simulation can be minimized by leaving the computation of these until after the FDTD simulation has been completed. Once the voxel SAR's have been computed the 1-g SAR is found by searching in a volume surrounding the peak voxel SAR. It should be noted that this volume should be sufficiently large; that the peak 1-g SAR is found as the center of this 1-g volume may not coincide with the peak voxel SAR.

Sinusoidal excitation is used to carrying out a simulation at fixed frequency with the peak E-fields being found during the final cycle of the simulation. A stable condition (i.e., when transient effects have decayed) is obtained typically after eight cycles. A convenient level of excitation (to give output values in a reasonable range) has been used and the resulting SAR values normalized using the sum of the power radiated from the FDTD grid and the power absorbed in the dielectrics. For the purposes of these simulations, the time-averaged power settings are 125 mW for 1900-MHz devices and 600 mW for 835-MHz devices.

Execution times for the parallel FDTD program simulating a mobile telephone next to a 1.974 mm $\times$ 1.974 mm $\times$ 3.0 mm head model (problem setup shown in Fig. 2) running on 1–16 processors are shown in Table I.

TABLE II
SAR DISTRIBUTIONS IN THREE ANATOMICALLY REALISTIC MODELS OF THE HUMAN HEAD WITH A PLASTIC-COVERED METAL BOX TELEPHONE OF DIMENSIONS 22.0 $\times$ 5.0 $\times$ 15.6 cm. THE SIMULATIONS HAVE BEEN CARRIED OUT AT 1900 MHz AND NORMALIZED TO 125 mW OF RADIATED POWER

	Model 1 1.974×1.974×3.0mm	Model 2 0.987×0.987×1.0mm Re-sampled from model 1	Model 3 0.9375mm^3
Peak 1-voxel SAR (W/kg)	5.88	10.97	6.77
Peak 1-g SAR (W/kg)	1.58	1.62	1.41
Peak 1-g SAR for Brain (W/kg)	0.27	0.26	0.32
Power Absorbed by head, neck and hand	58%	61.7%	61.5%
Brain Average SAR (mW/kg)	9.33	9.33	12.31
CSF Average SAR (mW/kg)	10.08	10.10	8.68
Lens average SAR (mW/kg)	1.17	1.17	1.612
Sclera Average SAR (mW/kg)	1.41	1.44	2.50
Humour Average SAR (mW/kg)	2.40	2.39	3.21

V. COMPARISON OF SAR DISTRIBUTION IN TWO ANATOMICALLY REALISTIC HEAD MODELS

Two head models described previously were used in a simulation with a generic (box-shaped) mobile telephone operating at a frequency of 1900 MHz. A quarter wave monopole antenna was used. The comparison of the results from 1.974 mm $\times$ 1.974 mm $\times$ 3.0 mm model and the same model resampled to 0.987 mm $\times$ 0.987 mm $\times$ 1.0 mm show the effect of changing resolution with essentially the same model. In these two simulations, the telephone is placed in the same position, determined by the location of the ear canal. A third simulation has been carried out using the alternate head model (with a voxel size of 0.9375 mm along each of the orthogonal axes), with the telephone again being positioned correctly with respect to the ear canal. The SAR distributions are given in Table II.

The SAR distributions for the 1.974 mm $\times$ 1.974 mm $\times$ 3.0 mm model and the sample model resampled to 0.987 mm $\times$ 0.987 mm $\times$ 1.0 mm are very similar. This would normally be expected (as the models are essentially the same but at different resolutions), however, it does prove the validity of the lower resolution model for simulations at 1900 MHz. The prediction of the peak 1-g averaged SAR using the 0.9375 mm^3 model is again very similar to that found from the other two models.

It should be noted that the 0.9375 mm^3 model has a much smaller ear. A consequence of this is that it is more difficult to accurately position the telephone next to the head.

VI. COMPARISONS OF SAR DISTRIBUTIONS USING A CAD TELEPHONE AND A PLASTIC-COVERED BOX TELEPHONE

Results of simulations using a plastic-covered box telephone (2.0 $\times$ 5.8 $\times$ 13.5 cm) and a CAD telephone (with both $\lambda/4$ and $3\lambda/8$ monopole antennas) at 835 MHz are given in Table III. These show that at 835 MHz the telephone derived from a CAD file and a simple box telephone are not dissimilar. However, it is a somewhat easier process to

TABLE III
SAR DISTRIBUTIONS FOR THE UTAH HEAD MODEL (1.974 mm × 1.974 mm × 3.0 mm, TILTED TO A REALISTIC POSITION) WITH A BOX TELEPHONE AND A CAD DERIVED TELEPHONE, AT 835 MHz. (NO HAND) RESULTS ARE NORMALIZED TO A 600 mW OF RADIATED POWER

	Box Telephone λ/4 Antenna	CAD Telephone λ/4 Antenna	CAD Telephone 3λ/8 Antenna
Peak 1-voxel SAR (W/kg)	11.355	8.99	6.54
Peak 1-g SAR (W/kg)	2.39	2.17	1.62
Peak 1-g SAR for Brain (W/kg)	0.81	0.64	0.78
Power Absorbed by head and neck	44.5%	41.0%	32.1%
Brain Average SAR (mW/kg)	60.24	51.38	50.49
CSF Average SAR (mW/kg)	69.39	61.05	60.66
Lens average SAR (mW/kg)	11.39	10.57	8.26
Sclera Average SAR (mW/kg)	15.93	15.17	10.96
Humour Average SAR (mW/kg)	27.69	27.09	19.57

TABLE IV
SAR DISTRIBUTIONS FOR THE UTAH HEAD MODEL (1.974 mm × 1.974 mm × 3.0 mm, TILTED TO A REALISTIC POSITION) WITH A BOX TELEPHONE AND A CAD DERIVED TELEPHONE, AT 1900 MHz (NO HAND). RESULTS ARE NORMALIZED TO A 125-mW TRANSMITTER

	Box Telephone λ/4 Antenna	CAD Telephone λ/4 Antenna (with buttons)	CAD Telephone 3λ/8 Antenna (with buttons)	CAD Telephone 3λ/8 Antenna (without buttons)
Peak 1-voxel SAR (W/kg)	8.59	6.25	5.88	5.89
Peak 1-g SAR (W/kg)	1.48	1.45	0.57	0.57
Peak 1-g SAR for Brain (W/kg)	0.15	0.16	0.18	0.18
Power Absorbed by head and neck	39.1%	34.5%	29.8%	29.8%
Brain Average SAR (mW/kg)	7.72	7.96	8.85	8.85
CSF Average SAR (mW/kg)	10.12	10.16	13.91	13.92
Lens average SAR (mW/kg)	2.40	1.98	0.94	0.94
Sclera Average SAR (mW/kg)	2.95	2.55	1.23	1.22
Humour Average SAR (mW/kg)	5.68	5.37	2.44	2.44

input the description of the telephone using the CAD file. It should be noted that consistently lower SAR values have been found using the CAD file telephone. This can be explained by reduced contact with the head due to the contoured shape of the CAD telephone. As expected [11], the peak 1-voxel and 1-g averaged SAR values using a $3\lambda/8$ monopole antenna are much lower than that using the $\lambda/4$ monopole antenna.

Similar results from simulations at 1900 MHz, are given in Table IV. It can be seen that results from the CAD telephone and the box telephone are very similar to those at 835 MHz (Table III) and once again the power absorbed is lower. Again this can be explained by the shaped profile of the CAD-derived telephone. This would also explain why the 1-g averaged SAR values are similar, as these are found as an average around this area of contact. As previously observed [10], [11], here too, the use of a $3\lambda/8$ monopole shows significantly lower peak 1-voxel and 1-g averaged SAR values. Although all simulations that used a CAD-derived telephone have used one that includes buttons (each simulated by a 10-mm-thick plastic of $\varepsilon_r = 4.0$ that protrudes 2.0 mm above the box), Table IV also shows a CAD-derived telephone without buttons. As expected, the effect of the buttons is negligible.

TABLE V
SAR DISTRIBUTIONS IN THE UTAH HEAD MODEL (1.974 mm × 1.974 mm × 3.0 mm, TILTED TO A REALISTIC POSITION) WITH A SHORTENED BOX TELEPHONE AND A SHORTENED BOX TELEPHONE WITH A REASONANT ELEMENT (A $\lambda/2$ DIPOLE) IMMEDIATELY BELOW IT AT 1900 MHz (NO HAND). RESULTS ARE NORMALIZED TO A 125-mW TRANSMITTER

	Short Box Telephone	Short Box Telephone with resonant element below
Peak 1-voxel SAR (W/kg)	5.60	6.00
Peak 1-g SAR (W/kg)	1.57	1.58
Peak 1-g SAR for Brain (W/kg)	0.21	0.21
Power Absorbed by head and neck	42.1%	42.49%
Brain Average SAR (mW/kg)	6.96	7.05
CSF Average SAR (mW/kg)	8.39	8.39
Lens average SAR (mW/kg)	1.43	1.43
Sclera Average SAR (mW/kg)	1.88	1.88
Humour Average SAR (mW/kg)	3.30	3.30

It is suggested that in reality the plastic mobile telephone may not be sufficiently metalized to prevent EM fields penetrating the box. It is also possible that resonant elements may exist within the digital circuits of the device. In order to determine the effects that these circuits may have upon the SAR distributions a simulation using a shortened metal box ($1.8 \times 5.4 \times 4.5$ cm) has been carried out at 1900 MHz. This box is of a similar size to that of the RF units inside a commercial mobile telephone. The remaining part of the device is modeled as a plastic box ($2.0 \times 5.8 \times 13.5$ cm). A $\lambda/4$ monopole antenna was used. A second simulation with a resonant element (a half-wave dipole resonant at 1900 MHz) inside the plastic box immediately below (one FDTD cell) the metal box and at the side closest to the head is also shown in Table V. As can be seen, the effect of the resonant element is minimal. However, the effect of shortening the box is more significant. Although the external dimensions of the telephone are the same as those used previously, somewhat higher 1-g SAR values are found (1.57 versus 1.48 W/kg). This is likely to be due to the increased field concentration surrounding the smaller box.

VII. CONCLUSIONS

Results have been presented that compare the SAR distribution in two anatomically accurate models of the human head. One of these models has been oversampled to provide a high-resolution equivalent, which has been used to show that negligible change is obtained for 1900-MHz simulations (i.e., a resolution than $1.974 \times 1.974 \times 3.0$ mm is not required at 1900 MHz). A model derived from MRI scans of a second volunteer have shown only minimal differences in the peak 1-g SAR values.

Second, all these simulations have been carried out using a parallel FDTD program, which has provided a number of advantages. First, simulations using the lower resolution model could be carried out quickly in a matter of minutes as opposed to hours. Second, simulations using the two higher resolution models would not have been possible, if this type of technology were not available. Although it has been demonstrated that a higher resolution model is not necessary

for SAR predictions at 1900 MHz, it will be necessary to simulate devices operating at even higher frequencies as they are introduced. Additionally, in order to prove that the lower resolution model provided sufficient accuracy it was necessary to make comparisons with a higher resolution model.

A method of taking CAD design files and using them as the basis of a model to be used in the FDTD program has been introduced. This saves a great deal of time in the modeling of many such devices. It also provides for a more accurate representation of the device and should inspire greater confidence in the numerical prediction of SAR distributions. Additionally, the effect of resonant elements within the telephone has been investigated and shown to have very little effect on the SAR distributions for the region of highest EM absorption close to the antenna.

ACKNOWLEDGMENT

The authorswould like to thank M. Pernice for his contributions in the parallelizing of the FDTD code.

REFERENCES

[1] ANSI/IEEE C95.1-1992, *American National Standard-Safety Levels with Respect to Exposure to Radio Frequency Electromagnetic Fields: 3 kHz to 300 GHz.* New York: IEEE, 1992

[2] Federal Communications Commission, "RE: Guidelines for evaluating the environmental effects of radio frequency radiation," FCC 96-326, Aug. 1, 1996.

[3] A. Taflove, *Computational Electrodynamics: The Finite-Difference Time-Domain Method*. Dedham, MA: Artech House, 1995.

[4] O. P. Gandhi, "Some numerical methods for dosimetry: Extremely low frequencies to microwave frequencies," *Radio Sci.*, vol. 30, pp. 161–177, 1995.

[5] C. Gabriel, "Compilation of the dielectric properties of body tissues at RF and microwave frequencies," Final Tech. Rep. AL/OE-TR-1996-0037, Occupat. Environmental Health Directorate, RFR Div., Brooks AFB, TX, June 1996.

[6] O. P. Gandhi and J. Y. Chen, "Electromagnetic absorption in the human head from experimental 6-GHz hand-held transceivers," *IEEE Trans. Electromagn. Compat.*, vol. 37, pp. 547–558, Nov. 1995.

[7] P. J. Dimbylow and S. A. Mann, "SAR calculations in an anatomically based realistic model of the head for mobile communication transceivers at 900 and 1800 MHz," *Phys. Med. Biol.*, vol. 39, pp. 1537–1553, 1994.

[8] M. A. Jensen and Y. Rahmat-Samii, "EM interaction of handset antennas and a human in personal communication," *Proc. IEEE*, vol. 83, pp. 7–17, 1995.

[9] G. Lazzi and O. P. Gandhi, "On modeling and personal dosimetry of normal mode helical antennas with the FDTD code," *IEEE Antennas Propagat.*, vol. 46, pp. 525–530, Apr. 1998.

[10] O. P. Gandhi, J. Y. Chen, and D. Wu, "Electromagnetic absorption in the human head for mobile telephones at 835 and 1900 MHz," in *Proc. Int. Symp. Electromagn. Compat.*, Rome, Italy, Sept. 1994, pp. 1–5.

[11] O. P. Gandhi, G. Lazzi, and C. M. Furse, "Electromagnetic absorption in the human head and neck for mobile telephones at 835 and 1900 MHz," *IEEE Trans. Microwave Theory Tech.*, vol. 44, pp. 1884–1897, Oct. 1996.

[12] G. Lazzi and O. P. Gandhi, "Realistically tilted and truncated anatomically based models of the human head for dosimetry of mobile telephones," *IEEE Trans. Electromagn. Compat.*, vol. 39, pp. 55–61, Feb. 1997.

[13] IRCP Publication 23, *Report of the Task Group on Reference Man*. New York: Pergamon, 1992.

Adam D. Tinniswood was born in Colne, U.K., in September 1968. He received the B.Sc. and D.Phil. degrees from the University of York, U.K., in 1991 and1996, respectively.

He worked for British Aerospace Preston, U.K, for two years. From September 1994 to June 1996 he worked at the University of Bradford, U.K., using the FDTD method coupled with parallel processing techniques, to solve large-scale bioelectromagnetic problems. He is now a Research Assistant Professor at the University of Utah, Salt Lake City, where he continues to investigate bioelectromagnetic effects.

Dr. Tinniswood won the International Union of Radio Science (URSI) Young Scientist Award in 1996.

Cynthia M. Furse was born in Stillwater, ME, on May 7, 1963. She received the B.S.E.E. and Ph.D. degrees from the University of Utah, Salt Lake City, in 1988 and 1994, respectively.

She has worked as a Research Assistant and Associate and Research Assistant Professor at the University of Utah from 1989 to 1997. She is currently an Assistant Professor at Utah State University, Logan, UT. Her research interests include applying numerical methods to electromagnetic interaction problems, parallel computation for large-scale applications, and high-resolution modeling of the human body for both low- and high-frequency bioelectromagnetic applications.

Om P. Gandhi (S'57–M'58–SM'65–F'79) received the B.Sc. (honors) degree in physics from Delhi University, Delhi, India, and the M.S.E. and Sc.D. degrees in electrical engineering from the University of Michigan, Ann Arbor.

He is a Professor and Chairman of the Department of Electrical Engineering, University of Utah, Salt Lake City. He is the author and coauthor of several book chapters and journal articles on electromagnetic dosimetry, microwave tubes, and solid-state devices. He also edited *Biological Effects and Medical Applications of Electromagnetic Energy* (Englewood Cliffs, NJ: Prentice-Hall, 1990) and coedited *Electromagnetic Biointeraction* (New York: Plenum, 1989).

Dr. Gandhi received the Distinguished Research Award from the University of Utah for 1979–1980. He has been the President of the Bioelectromagnetics Society (1992–1993), co-chairman of the IEEE SCC 28.IV Subcommittee on the RF Safety Standards (1988 to the present), and chairman of the IEEE Committee on Man and Radiation (COMAR) for 1980–1982. In 1995 he received the d'Arsonval Medal of the Bioelectromagnetics Society for pioneering contributions to the field of bioelectromagnetics. His name is listed in *Who's Who in the World*, *Who's Who in America*, *Who's Who in Engineering*, and *Who's Who in Technology Today*.